Adaptive master-slave cubature Kalman filters subject to state inequality constraints for wind turbine state estimation

Ritter, B.; Mora, E.; Schild, A.; Doekemeijer, B. M.; Konigorski, U.

DOI
10.23919/acc.2019.8814411

Publication date
2019

Document Version
Final published version

Published in
Proceedings of the 2019 American Control Conference (ACC 2019)

2019 American Control Conference (ACC)
Philadelphia, PA, USA, July 10-12, 2019

Adaptive Master-Slave Cubature Kalman Filters subject to State Inequality Constraints for Wind Turbine State Estimation

B. Ritter[1,2], E. Mora[1‡], A. Schild[3], B.M. Doekemeijer[4] and U. Konigorski[1]

***Abstract*— The cubature Kalman filter (CKF) is well-known for a decade as a derivative-free nonlinear Kalman filter that is well-suited for high-dimensional nonlinear estimation problems. This paper further develops this classical CKF in order to cope with time-varying noise statistics as well as inequality constraints on the estimated states. The resulting adaptive filter is suggested to provide more accurate state estimates and to be more robust against filter divergence. Moreover, this contribution proposes an automated filter design based on numerical optimization which uses the normalized estimation error squared (NEES) and the normalized innovation squared (NIS) as part of the objective function. The novel adaptive CKF is applied to wind turbines in order to assess the potential improvement for state and parameter estimation. The simulation results for an illustrative acid test scenario with time-varying measurement noise show the superiority of the novel adaptive CKF since it compensates the noise robustly and thereby outperforms the classical filter.**

I. INTRODUCTION

The cubature Kalman filter (CKF) is a derivative-free filter for nonlinear systems [1]. It is the latest family member of the so-called sigma-point Kalman filters (SPKF) which are said to be superior to the widely used extended Kalman filter (cf. [2]–[4]). Although the classical CKF deals readily with nonlinear systems, it cannot cope with undetected changes in noise statistics and state constraints which both constitute relevant issues in practice. Previous studies have found the master-slave adaptive approach, originally introduced by Song et al. [5], to be advantageous for noise adaptation since critical parameters are freely selectable and computational costs increase only moderately [6]. Contrary to the linear slave KF by Qi et al. [7], this paper proposes a novel version which allows to adapt optionally both covariance matrices and which does not require the pseudo inverse of the Kalman gain to be computed. Additionally, this master-slave filter is enhanced by a projection approach [8] to manage the inequality constraints for the estimated states and parameters.

As an application example, multi-megawatt wind turbines are investigated in this paper. The reason is that advanced model-based controllers like nonlinear model predictive control (NMPC) have shown a promising potential to mitigate component loads and to increase energy yield (e.g. [9]–[12]). Though, these controllers require the complete state vector as *measurements* in order to outperform standard industrial wind turbine control [13], [14]. The proposed adaptive filter is employed in order to ensure the availability of accurate state estimates under unknown noise statistics at any time.

The remainder of this paper is structured as follows: First, the adaptive Kalman filter with state constraints is introduced in Section II. Then, the automatic filter design is presented in Sect. III and the simplified wind turbine model is established in Sect. IV. After that, the test scenario and the illustrative simulation results are discussed in Sect. V and the main outcomes are summarized in Sect. VI.

II. ADAPTIVE CUBATURE KALMAN FILTER WITH STATE CONSTRAINTS

The structure of the novel adaptive filter is shown in Fig. 1. It consists of a classical CKF with constraints handling as

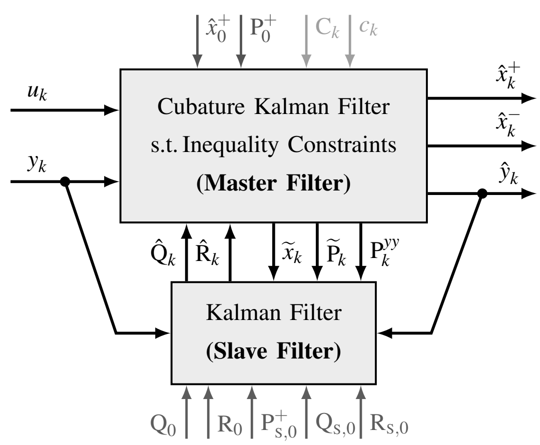

Fig. 1. Structure of the master-slave CKF for process and/or measurement noise adaptation with state constraints (left: KF inputs, right: KF estimates, dark gray: free filter parameters, light gray: constraint parameters)

master filter and a linear KF as slave filter. The different parts are introduced hereafter.

A. The Cubature Kalman Filter Algorithm

The CKF propagates $2n_x$ deterministically chosen sigma-points (SP) through the process model $f(\cdot)$ and then through the output model $h(\cdot)$ where n_x is the number of states (cf. [1]). The algorithm reads:

[1]Bastian Ritter and Ulrich Konigorski are with the Institute of Automatic Control and Mechatronics, Dept. of Control Systems and Mechatronics, Technische Universität Darmstadt, Landgraf-Georg-Str. 4, 64283 Darmstadt, Germany, ‡ Edwin Mora is now with the Dept. of Energy Information Networks and Systems (same university), correspond to: britter@iat.tu-darmstadt.de

[2]Bastian Ritter is also with the Industrial Science GmbH powered by IAV, Alexanderstr. 25, 64283 Darmstadt, Germany

[3]Axel Schild is with the IAV GmbH, Rockwellstraße 16, 38518 Gifhorn, Germany

[4]Bart Matthijs Doekemeijer is with the Delft Center for Systems and Control (DCSC), Faculty of Mechanical Engineering, Delft University of Technology, Mekelweg 2, 2628 CD Delft, The Netherlands

1) Initialization Step:

$$\hat{x}_0^+ = E\{x_0\} \tag{1a}$$

$$\mathrm{P}_0^+ = E\{(x_0 - \hat{x}_0^+)(x_0 - \hat{x}_0^+)^{\mathrm{T}}\} \tag{1b}$$

2) Prediction Step for $k > 0$:

$$\boldsymbol{\mathcal{X}}_{k-1}^+ = \widehat{\mathrm{X}}_{k-1}^+ + \left(\sqrt{2n_x}\right)^{-1}\left[\sqrt{\mathrm{P}_{k-1}^+}, -\sqrt{\mathrm{P}_{k-1}^+}\right] \tag{2a}$$

$$\boldsymbol{\mathcal{X}}_k^* = f(\boldsymbol{\mathcal{X}}_{k-1}^+, u_{k-1}) \tag{2b}$$

$$\hat{x}_k^- = (2n_x)^{-1}\sum_{i=1}^{2n_x}\boldsymbol{\mathcal{X}}_k^*(:,i) \tag{2c}$$

$$\mathrm{P}_k^- = (2n_x)^{-1}\boldsymbol{\mathcal{X}}_k^*\left(\boldsymbol{\mathcal{X}}_k^*\right)^{\mathrm{T}} - \hat{x}_k^-\left(\hat{x}_k^-\right)^{\mathrm{T}} + \mathrm{Q}_{k-1} \tag{2d}$$

$$\boldsymbol{\mathcal{X}}_k^- = \widehat{\mathrm{X}}_k^- + \left(\sqrt{2n_x}\right)^{-1}\left[\sqrt{\mathrm{P}_k^-}, -\sqrt{\mathrm{P}_k^-}\right] \tag{2e}$$

$$\boldsymbol{\mathcal{Y}}_k^* = h\left(\boldsymbol{\mathcal{X}}_k^-, u_k\right) \tag{2f}$$

$$\hat{y}_k = (2n_x)^{-1}\sum_{i=1}^{2n_x}\boldsymbol{\mathcal{Y}}_k^*(:,i) \tag{2g}$$

3) Correction Step for $k > 0$:

$$\mathrm{P}_k^{xy} = (2n_x)^{-1}\boldsymbol{\mathcal{X}}_k^*\left(\boldsymbol{\mathcal{Y}}_k^*\right)^{\mathrm{T}} - \hat{x}_k^-\left(\hat{y}_k\right)^{\mathrm{T}} \tag{3a}$$

$$\mathrm{P}_k^{yy} = (2n_x)^{-1}\boldsymbol{\mathcal{Y}}_k^*\left(\boldsymbol{\mathcal{Y}}_k^*\right)^{\mathrm{T}} - \hat{y}_k\left(\hat{y}_k\right)^{\mathrm{T}} + \mathrm{R}_k \tag{3b}$$

$$\boldsymbol{\mathcal{K}}_k = \mathrm{P}_k^{xy}\left(\mathrm{P}_k^{yy}\right)^{-1} \tag{3c}$$

$$\hat{x}_k^+ = \hat{x}_k^- + \boldsymbol{\mathcal{K}}_k\left(y_k - \hat{y}_k^-\right) = \hat{x}_k^- + \boldsymbol{\mathcal{K}}_k v_k \tag{3d}$$

$$\mathrm{P}_k^+ = \mathrm{P}_k^- + \boldsymbol{\mathcal{K}}_k \mathrm{P}_k^{yy}\boldsymbol{\mathcal{K}}_k^{\mathrm{T}} \tag{3e}$$

The Eq. (3d) is denoted as update equation where $\hat{x}_k^-$ and the innovation v_k are weighted according to the Kalman gain $\boldsymbol{\mathcal{K}}_k$. The CKF's only design parameters are the covariance matrices Q_k and R_k of the additive process and measurement noises (both assumed diagonal). Remarks: $\hat{x}_k^-$ and $\hat{x}_k^+$ are the a priori/posterior state estimates. P_k^- and P_k^+ are the a priori/posterior error covariances, P_k^{yy} and P_k^{xy} the innovation/cross covariances, $\boldsymbol{\mathcal{X}}_{k-1}^+$ and $\boldsymbol{\mathcal{X}}_k^-$ are the SP before propagation, $\boldsymbol{\mathcal{X}}_k^*$ and $\boldsymbol{\mathcal{Y}}_k^*$ after propagation. u_k and y_k are the control inputs and outputs (cf. [14] for a more detailed notation).

B. The slave Kalman filter

The slave filter is realized as a linear KF since both the process and the output model are linear. The symbol S labels the slave filter variables. The slave state vector is denoted as $x_{\mathrm{S},k}$ which contains the diagonal elements of the process or measurement noise (or both). The algorithm denotes:

1) Initialization Step:

$$\hat{x}_{\mathrm{S},0}^+ = E\{x_{\mathrm{S},0}\} \tag{4a}$$

$$\mathrm{P}_{\mathrm{S},0}^+ = E\left\{(x_{\mathrm{S},0} - \hat{x}_{\mathrm{S},0}^+)(x_{\mathrm{S},0} - \hat{x}_{\mathrm{S},0}^+)^{\mathrm{T}}\right\} \tag{4b}$$

2) Prediction Step for $k > 0$:

$$\hat{x}_{\mathrm{S},k}^- = \hat{x}_{\mathrm{S},k-1}^+ \tag{5a}$$

$$\mathrm{P}_{\mathrm{S},k}^- = \mathrm{P}_{\mathrm{S},k-1}^+ + \mathrm{Q}_{\mathrm{S},0} \tag{5b}$$

$$\hat{y}_{\mathrm{S},k} = \hat{x}_{\mathrm{S},k}^- + u_{\mathrm{S},k} \tag{5c}$$

3) Correction Step for $k > 0$:

$$\mathrm{P}_{\mathrm{S},k}^{xy} = \mathrm{P}_{\mathrm{S},k}^- \tag{6a}$$

$$\mathrm{P}_{\mathrm{S},k}^{yy} = \mathrm{P}_{\mathrm{S},k}^- + \mathrm{R}_{\mathrm{S},0} \tag{6b}$$

$$\boldsymbol{\mathcal{K}}_{\mathrm{S},k} = \mathrm{P}_{\mathrm{S},k}^{xy}\left(\mathrm{P}_{\mathrm{S},k}^{yy}\right)^{-1} \tag{6c}$$

$$\hat{x}_{\mathrm{S},k}^+ = \hat{x}_{\mathrm{S},k}^- + \boldsymbol{\mathcal{K}}_{\mathrm{S},k}(y_{\mathrm{S},k} - \hat{y}_{\mathrm{S},k}) \tag{6d}$$

$$\mathrm{P}_{\mathrm{S},k}^+ = \mathrm{P}_{\mathrm{S},k}^- - \boldsymbol{\mathcal{K}}_{\mathrm{S},k}\mathrm{P}_{\mathrm{S},k}^{yy}\boldsymbol{\mathcal{K}}_{\mathrm{S},k}^{\mathrm{T}} \tag{6e}$$

Theoretically, Q_k and R_k can be adapted simultaneously. However, the resulting filter is not robust since it is hard to distinguish between errors in both matrices [15] (p. 44). That is why the state vector $x_{\mathrm{S},k}$ is proposed as either $x_{\mathrm{S},k} = q_k(i_Q)$ or $x_{\mathrm{S},k} = r_k(i_R)$ where $q_k = \mathrm{diag}\{\mathrm{Q}_k\}$ and $r_k = \mathrm{diag}\{\mathrm{R}_k\}$. The vectors i_Q and i_R select the entries to be adapted.

The definitions of the outputs $y_{\mathrm{S},k}$ and the inputs $u_{\mathrm{S},k}$ in Eqs. (5c) and (6d) depend on the chosen noise parameters:

$$y_{\mathrm{S},k} = \mathrm{diag}\left\{\frac{1}{N}\sum_{i=i_0}^{k} v_i v_i^{\mathrm{T}}\right\},\ u_{\mathrm{S},k} = \mathrm{diag}\left\{\mathrm{P}_k^{yy} - \hat{\mathrm{R}}_{k-1}\right\} \tag{7}$$

$$y_{\mathrm{S},k} = \mathrm{diag}\left\{\frac{1}{N}\sum_{i=i_0}^{k} \tilde{x}_i \tilde{x}_i^{\mathrm{T}}\right\},\ u_{\mathrm{S},k} = \mathrm{diag}\left\{\widetilde{\mathrm{P}}_k - \hat{\mathrm{Q}}_{k-1}\right\} \tag{8}$$

wherein $\widetilde{\mathrm{P}}_k = \mathrm{P}_k^- - \mathrm{P}_k^+$ and $i_0 = k - N + 1$. Eq. (7) is used for adaptation of R_k based on the innovation $v_k = y_k - \hat{y}_k^-$ and Eq. (8) for Q_k based on the state residual $\tilde{x}_k = \hat{x}_k^+ - \hat{x}_k^-$. The outputs $y_{\mathrm{S},k}$ correspond to the diagonal elements of the sample innovation or residual covariance matrix. The free design parameters are i_Q, i_R, N, $\mathrm{Q}_{\mathrm{S},0}$ and $\mathrm{R}_{\mathrm{S},0}$.

C. State Inequality Constraints

The state of real-world systems is always confined to an allowable region due to physical constraints. These are determined by box constraints $x_{\min} \le x_k \le x_{\max}$, which read in a general form (denoted as state inequality constraints)

$$\mathrm{C}_k x_k \le c_k\ . \tag{9}$$

If these constraints are violated, this constitutes a problem when applied to the feedback controller and thus an algorithm to restrict the estimates is needed. In this paper, a concept proposed by Kandepu et al. [8] is employed where the SP are projected to a feasible region defined by Eq. (9). Accordingly, Eqs. (2a) and (2b) are extended by

$$\boldsymbol{\mathcal{X}}_{k-1}^{+,\mathrm{c}} = P(\boldsymbol{\mathcal{X}}_{k-1}^+) \tag{10a}$$

$$\boldsymbol{\mathcal{X}}_k^{*,\mathrm{c}} = P(\boldsymbol{\mathcal{X}}_k^*) \tag{10b}$$

where P represents the projection onto the region. Concluding, the main advantages of this approach are its simplicity, its practicability for sigma-point filters and the fact that both, the mean and the covariance, are affected by the state constraints at the same time.

III. AUTOMATED FILTER DESIGN

Filter design is referred to as the process of selecting the free filter parameters such that the estimation performance is optimized with respect to an objective function or performance criterion. This is sometimes denoted as *tuning process* when parameters are manually designed by expert knowledge. Unfortunately, this process becomes very cumbersome (and on a trial and error basis) with increasing number of estimated states and free parameters. Therefore, an automated filter design is desirable to ease the application and also to optimize the filter performance. This is done by defining and solving an optimization problem.

A. Performance Measures

In order to assess the filter performance, the estimation error e_k (EE) and the innovation v_k are defined as follows:

$$e_k = x_k - \hat{x}_k^+ \quad \text{and} \quad v_k = y_k - \hat{y}_k \,. \tag{11}$$

While the first is only available in simulation, the second is also known in reality. Based on Eq. (11), the normalized estimation error squared (NEES) $\varepsilon_{\mathrm{NS},k}$ and the normalized innovation squared (NIS) $v_{\mathrm{NS},k}$ are derived to assess the filter consistency. The definitions read [16] (p. 165/p. 236):

$$\varepsilon_{\mathrm{NS},k} = e_k^{\mathrm{T}} \mathrm{M}_k^+ e_k \quad \Rightarrow \quad \varepsilon_{\mathrm{NS},k} \sim \chi^2_{n_x} \tag{12}$$

$$v_{\mathrm{NS},k} = v_k^{\mathrm{T}} \mathrm{M}_k^{yy} v_k \quad \Rightarrow \quad v_{\mathrm{NS},k} \sim \chi^2_{n_y} \tag{13}$$

The NEES and NIS are χ^2-distributed with n_x or n_y degrees of freedom. n_y is the number of outputs. M_k^+ and M_k^{yy} are the matrix inverses of P_k^+ and P_k^{yy}, respectively. It is well known that filter consistency implies that

$$E\{\varepsilon_{\mathrm{NS},k}\} = n_x \quad \text{and} \quad E\{v_{\mathrm{NS},k}\} = n_y \tag{14}$$

must hold [16] (p. 59). Eqs. (14) can be statistically used as

$$\bar{\varepsilon}_{\mathrm{NS}} = \frac{1}{n_x M} \sum_{k=1}^{M} \varepsilon_{\mathrm{NS},k} \quad \text{and} \quad \bar{v}_{\mathrm{NS}} = \frac{1}{n_y M} \sum_{k=1}^{M} v_{\mathrm{NS},k} \tag{15}$$

which are the *normalized* sample means (obtained for a sufficiently large number of samples M to capture the statistics correctly). Hence, the filter is said to be consistent when

$$\bar{\varepsilon}_{\mathrm{NS}} \approx 1 \quad \text{and} \quad \bar{v}_{\mathrm{NS}} \approx 1 \tag{16}$$

holds. To put it simple, consistency ensures that the filter is always aware of how reliable its estimates actually are [17].

B. Objective Function and Optimization Problem

Based on the above, the objective function to assess the filter's performance is proposed as follows:

$$J(z) = w \log\big(\bar{\varepsilon}_{\mathrm{NS}}(z)\big)^2 + (1-w) \log\big(\bar{v}_{\mathrm{NS}}(z)\big)^2 \tag{17}$$

where z contains the free design parameters (defined in Sect. III-C). The weighting factor $w \in [0,1]$ allows to put emphasis either on the NEES (if the true states are known from advanced measurement configurations or in simulation) or on the NIS (if true states are unknown).

The objective function Eq. (17) has three advantages: First, it ensures that pessimism and optimism in filter tuning [17] are weighted equally (cf. Fig. 2). Secondly, there are no tuning parameters since the weights are predefined by the filter covariance matrices in Eqs. (12) and (13). This is different compared to an alternative objective function in [18] where weighting matrices are chosen manually. Thirdly,

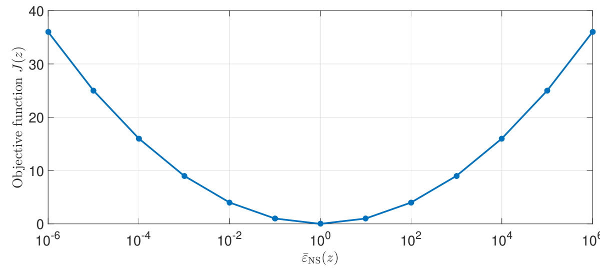

Fig. 2. $J(\bar{\varepsilon}_{\mathrm{NS}}(z))$ as function of the normalized NEES ($w = 1$)

Eq. (17) provides a statistically consistent estimator when the optimum J^* is found.

Based on the above considerations, the generic optimization problem (OP) for an automated design is stated as follows:

$$\begin{aligned} &\min_{z} J(z) \quad \rightarrow \text{Eq. (17)} \\ &\text{s.t. } [\hat{x}_i^+, \hat{y}_i] = \mathrm{F}(z, u_i, y_i) \;:\; \forall i \in [1, 2, \dots, M] \\ &\quad \underline{z} \leq z \leq \bar{z} \end{aligned} \tag{18}$$

Therein, $\mathrm{F}(\cdot)$ represents the chosen filter algorithm (here the CKF or MS-CKF). The optimization variables z are limited by lower bounds $\underline{z}$ and upper bounds $\bar{z}$.

C. Approach to Automated Filter Design

Automated design is conceived as finding the *right* filter parameter configuration with little manual interference. For this reason, the optimization is done with a set of training data (simulation results) that is processed steadily through the filter. After that, the filter outputs are evaluated using Eq. (17). When the optimization is completed, the performance is assessed with simulation data from different test scenarios (cf. Sect. V-C).

A three-step approach is proposed to achieve an optimal design:

1) Optimize the CKF initial parameters: The first optimization problem serves to find suitable design parameters for the standard CKF. Thus, $\mathrm{F}(\cdot) = \mathrm{CKF}(\cdot)$ and $z = [q_0^{\mathrm{T}}\, r_0^{\mathrm{T}}]^{\mathrm{T}}$ are chosen which are the initial diagonal elements of the covariance matrices.

2) Select the Noise Covariances: Once optimized covariance matrices Q_0^* and R_0^* are found, a sensitivity study is conducted to determine the noise parameters to be estimated for adaptation. For instance, $i_Q = [\,]^{\mathrm{T}}$ and $i_R = [1, 2, \dots, n_y]^{\mathrm{T}}$ are chosen for measurement noise adaptation. The number of samples N must be chosen appropriately. It must be large enough to assess the sample covariances in Eqs. (7) and (8) correctly, but not too large in order to react quickly enough.

3) Optimize the Slave Parameters: Afterwards, the second optimization problem aims to find the diagonal entries for the slave filter's covariance matrices. Thus, $\mathrm{F}(\cdot) = \text{MS-CKF}(\cdot)$ and $z = [q_{\mathrm{S},0}^{\mathrm{T}}\, r_{\mathrm{S},0}^{\mathrm{T}}]^{\mathrm{T}}$ are chosen.

This procedure can happen in a highly automated fashion and with only little expert input. Good starting values for the OPs are obtained either from expert knowledge or from a genetic algorithm. This improves the manual tuning process significantly and yields an optimally designed adaptive filter.

IV. CONTROL-ORIENTED MODELLING FOR WIND TURBINE STATE ESTIMATION

Today's modern wind turbines are large, resonating and flexible structures with multiple components that harvest together the energy from the alternating wind (cf. Fig. 3).

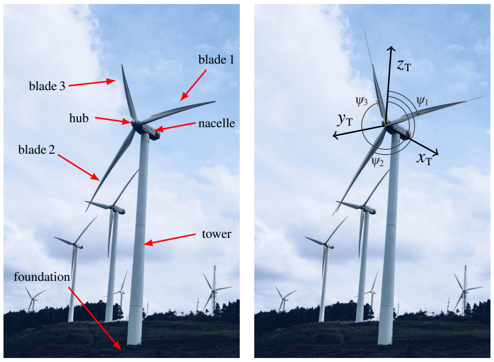

Fig. 3. Three-bladed wind turbine in a small wind farm within complex terrain (left: main components, right: variables and coordinate system)

When the complete system is modelled in greater detail (cf. high-fidelity simulators like FAST8 [19]), this involves many degrees-of-freedom. Such simulation models are accordingly complex and too detailed for control purposes.

A. The Design Model

Hence, the simplified design model incorporates only the relevant dynamics like the axial nacelle motion x_T and the drive-train rotation $\dot{\varphi}_\mathrm{g}$, and is derived from first principle approach (cf. [6], [20]). The dynamic model reads as follows:

$$\ddot{x}_\mathrm{T} = m_\mathrm{T}^{-1}\big(F_\mathrm{T}(\cdot) + \zeta M_\mathrm{n}(\cdot)\big) - 2\zeta_{\mathrm{T}x}\omega_0\dot{x}_\mathrm{T} - \omega_0^2 x_\mathrm{T} \tag{19a}$$

$$\ddot{\varphi}_\mathrm{g} = \Theta^{-1}\big(M_\mathrm{a}(\cdot) + i_\mathrm{gb}^{-1}M_\mathrm{g}\big) \tag{19b}$$

wherein the rotor thrust $F_\mathrm{T}(\cdot)$, the rotor torque $M_\mathrm{a}(\cdot)$ and the nodding moment $M_\mathrm{n}(\cdot)$ are defined according to

$$F_\mathrm{T} = \frac{\rho}{2}\frac{\pi R^2}{3}\sum_{b=1}^{3} C_\mathrm{T}\big(\lambda_b,\beta_b\big)v_b^2 \tag{20a}$$

$$M_\mathrm{a} = \frac{\rho}{2}\frac{\pi R^3}{3}\sum_{b=1}^{3} C_\mathrm{M}\big(\lambda_b,\beta_b\big)v_b^2 \tag{20b}$$

$$M_\mathrm{n} = \frac{\rho}{2}\frac{\pi R^2}{3}\sum_{b=1}^{3} r_\mathrm{n}(v_b)\cos\psi_b\, C_\mathrm{T}\big(\lambda_b,\beta_b\big)v_b^2\,. \tag{20c}$$

The nonlinearity is induced by the so-called aero-elastic coupling. It describes the interaction between the rotor blades and the inflow wind, causing nacelle and blades to oscillate which in turn affects the aerodynamic forces again. Moreover, the azimuth angle ψ_b, the tip-speed-ratio λ_b and the relative wind speed v_b for the blades $b \in [1,2,3]$ read

$$v_b = \big(1 + H^{-1}r_\mathrm{B}\cos\psi_b\big)^{\kappa}v_\mathrm{w} - \big(1 + \zeta r_\mathrm{B}\cos\psi_b\big)\dot{x}_\mathrm{T} \tag{21a}$$

$$\psi_b = \varphi_\mathrm{g} + 2\pi/3\,(b-1) \tag{21b}$$

$$\lambda_b = \dot{\varphi}_\mathrm{g} R\, {v_b}^{-1} \quad . \tag{21c}$$

In Eqs. (20), the aerodynamic coefficients for thrust $C_\mathrm{T}(\cdot)$ and torque $C_\mathrm{M}(\cdot)$ describe the simplified aerodynamics at the blades. Note that, m_T is the first modal mass, $\zeta_{\mathrm{T}x}$ the modal damping, ω_0 the first eigenfrequency, ζ the beam-coupling coefficient, ρ the air density, Θ the rotational drive-train inertia, i_gb the gear-box ratio, R the blade tip-radius, r_n the normal effective and r_B the power effective radii, H the hub height, $v_\mathrm{w}(t)$ the rotor-effective wind speed and $\kappa(t)$ the exponential shear coefficient (both unknown disturbances).

The model is multiple-input multiple-output and has the control inputs $u = [M_\mathrm{g}\ \beta_1\ \beta_2\ \beta_3]^\mathrm{T}$, being the generator torque M_g and the blade pitch angles β_b. The sensor outputs are $y = [n_\mathrm{g}\ \ddot{x}_\mathrm{T}\ \varphi_\mathrm{g}]^\mathrm{T}$, the generator speed $n_\mathrm{g} = 60/(2\pi)i_\mathrm{gb}\dot{\varphi}_\mathrm{g}$, the nacelle acceleration $\ddot{x}_\mathrm{T}$, and the azimuth angle φ_g.

B. Model Validation

Since model mismatches between the design model and real system may impair the estimator's performance, it must be verified in advance that the model parameters and model structure are correct. This has been done with FAST8 showing a very good agreement, cf. [18]. Additionally, field data from different 2 MW to 5 MW wind turbines was used to confirm the model's suitability.

V. SIMULATION RESULTS

For this simulation study the widely-used 5 MW reference turbine is considered as state-of-the-art wind turbine design. The model parameters were taken from [21]. The automated design approach with $w = 1$, as presented in Sect. III, has been applied to obtain the optimal filter parameters. In the following, this optimal design for the noise-free case is tested in a noisy measurement environment.

A. Test Scenario Description

The turbulent wind field in Fig. 4 with an average wind speed of $v_\mathrm{m} = 9\,\mathrm{m/s}$ and vertical shear of $\kappa = 0.2$ has been applied to the 5 MW wind turbine implemented in FAST8. The obtained simulation data is used to test the non-

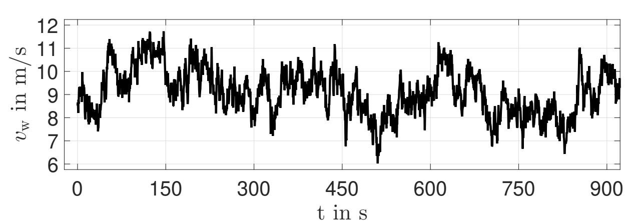

Fig. 4. Turbulent wind field in the wind turbine's partial load regime with an average wind speed $v_\mathrm{m} = 9\,\mathrm{m/s}$ and a turbulence intensity $\mathrm{TI} = 11\,\%$

adaptive CKF and adaptive filter MS-CKF extensively. The scenario investigates data for $T_\mathrm{SIM} = 900\,\mathrm{s}$ where the filter sample times are set to $T_\mathrm{S} = 0.1\,\mathrm{s}$. The length of the moving window for averaging the noise statistics is $T_N = 50\,\mathrm{s}$ and thus $N = 500$. For this problem, a range of $300 \leq N \leq 700$ is well suited to adapt R_k.

The noise adaptation of the MS-CKF is activated at $t = T_N$. Both filters are tested against the time-varying noisy signals, as shown in Fig. 5, where two critical measurements n_g and

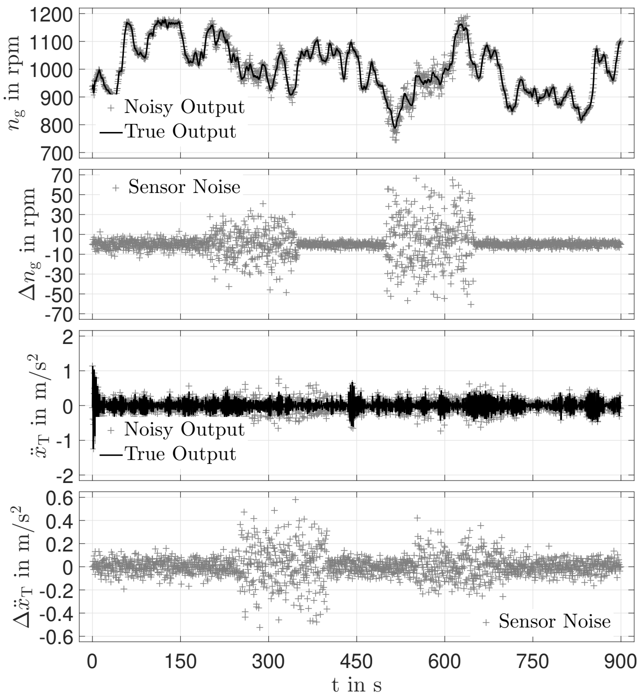

Fig. 5. Comparison of selected measurements with and w/o sensor noise

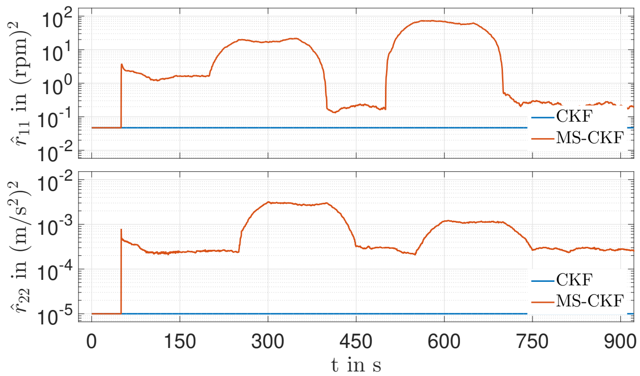

Fig. 6. Comparison of static and estimated sensor noise parameters

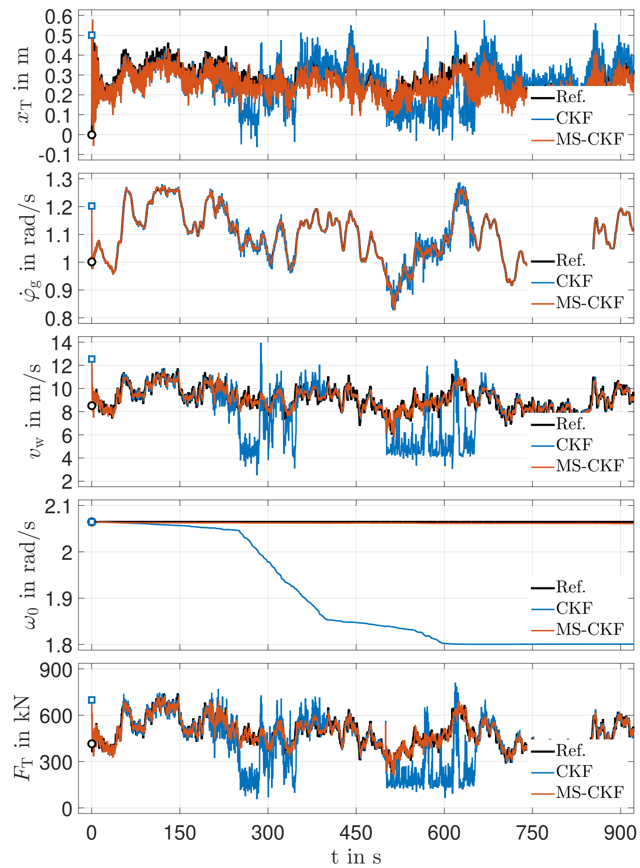

Fig. 7. Comparison of selected true and estimated quantities

$\ddot{x}_T$ are corrupted by zero-mean white Gaussian noise (with step changes in noise covariances).

B. Illustrative Estimation Problem

The CKF and MS-CKF receive the control inputs u and the noisy outputs y as information. The disturbances $v_w(t)$ and κ are completely unknown (since no wind measurements are available). The estimation problem is split as follows:

- The master filter estimates the states $x = [\dot{x}_T \; x_T \; \dot{\varphi}_g \; \varphi_g]^T$, the eigenfrequency ω_0 and the wind speed v_w using a monolithic CKF. Hence, an augmented system with the parameter models $\dot{\omega}_0 = 0$ and $\dot{v}_w = 0$ is included.
- The linear slave filter estimates the measurement noise covariances $r = [r_{11} \; r_{22} \; r_{33}]^T$ (diagonal elements of R_k). The process noise Q_k is assumed to be correct.

Thus, $n_x = 6$ and $n_y = 3$. Additionally, Eqs. (20) are used to compute estimates for the rotor thrust F_T and torque M_a.

C. Estimation Results

Due to limited space, only the most relevant quantities are shown in the following. First, Fig. 6 shows the measurement noise estimates for two noisy sensor signals. The MS-CKF follows quickly the changing noise covariances what the CKF cannot do. It takes only 50 s after each step to adapt to the new level which corresponds to the choice of T_N. The slave estimates $\hat{r}_{ii}$ are passed on to the master filter in case of the MS-CKF (cf. Fig. 1).

Fig. 7 shows illustratively the effect of the adaptation on the quality of the state estimates. It is observed that the CKF estimates are impaired by the increased sensor noise while the estimates of the adaptive filter remain almost unaffected. The CKF cannot react to the varying noise environment which leads at worst to divergence (e.g. for the wind speed estimate). The state constraints prevent the CKF from diverging to a non-physical region (the lower bounds are 4 m/s for v_w and 1.8 rad/s for ω_0). These constraints are the reason why the CKF is able to recover when the noise subsides to an acceptable level at $t = 350$ s and $t = 650$ s. Fig. 8 provides a quantitative comparison of the estimation errors.

In order to evaluate the success of the adaptation, Fig. 9 compares the diagonal elements of the innovation covariance matrices. It can be seen that the discrepancies between the sample and filter covariances for the CKF are completely eliminated by the adaptation (both are identical for the MS-CKF). Thus, the goal to match the covariance matrices has been perfectly achieved. These simulation results highlight the superiority of the MS-CKF over the standard CKF.

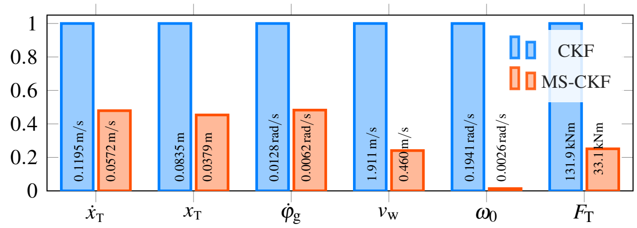

Fig. 8. Root mean-squared errors of estimated quantities (absolute values as numbers and normalized values with respect to CKF as bars)

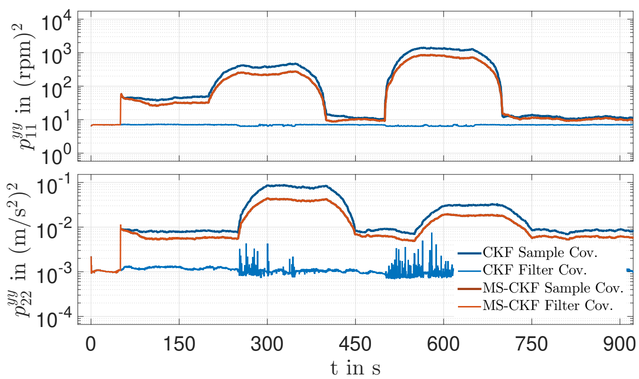

Fig. 9. Comparison of selected diagonal elements of the sample and the filter innovation covariance matrices

In a nutshell, noise adaptation and constraints handling make a significant difference in filter performance when it comes to dealing with uncertainties in practice. The designed MS-CKF tackles even step changes in noise statistics and adapts quickly. Thereby, it outperforms the standard CKF considerably.

VI. CONCLUSIONS

This contribution has introduced a novel, adaptive CKF that addresses filter adaptation and state constraints in nonlinear state estimation problems at the same time. Compared to earlier publications ([7], [18], [22]), this approach allows to adapt theoretically both covariance matrices for process and measurement noise at the same time. Moreover, this approach also ensures that state estimates do not leave their allowable region which as a by-product facilitates the recovery of a poorly designed filter when the temporary noise conditions subside to an acceptable level.

The paper has also proposed a promising design methodology that pursues the goal to facilitate a highly automated filter design. This automated design is based on the numerical solution of an optimization problem. The proposed filter specific objective function has the advantage that no tuning parameters have to be chosen (compared to [18]) as well as that, if and when the optimal design is found, this yields a consistent estimator by nature.

Finally, this contribution has assessed the non-adaptive and the novel adaptive CKF using an acid test scenario for wind turbine state estimation. The illustrative simulation results confirm that the novel adaptive filter has important properties which are required for an industry-ready application in wind turbine control and monitoring schemes.

Future work will investigate the identifiability problem of certain filter parameters and the effect on the filter performance. Additionally, the presented methodology extends to wind farm state estimation and is also applicable as part of advanced wind farm control schemes.

REFERENCES

[1] I. Arasaratnam and S. Haykin, "Cubature Kalman filters," *IEEE Transactions on Automatic Control*, vol. 54, no. 6, pp. 1254–1269, June 2009.

[2] S. J. Julier and J. K. Uhlmann, "Unscented filtering and nonlinear estimation," *Proceedings of the IEEE*, vol. 92, no. 3, pp. 401–423, March 2004.

[3] R. van der Merwe and E. A. Wan, "The square-root unscented Kalman filter for state and parameter-estimation," *IEEE International Conference on Acoustics, Speech, and Signal Processing, 2001. Proceedings. (ICASSP '01). 2001*, vol. 6, pp. 3461–3464, 2001.

[4] R. van der Merwe, "Sigma-point Kalman filters for probabilistic inference in dynamic state-space models," Ph.D. dissertation, Oregon Health & Science University, 2004.

[5] Q. Song, Z. Jiang, and J. Han, "Noise covariance identification based adaptive UKF with application to mobile robot systems," in *2007 IEEE International Conference on Robotics and Automation*, 2007.

[6] B. Ritter, E. Mora, T. Schlicht, A. Schild, and U. Konigorski, "Adaptive sigma-point Kalman filtering for wind turbine state and process noise estimation," *Journal of Physics: Conf. Series*, vol. 1037, no. 032003, pp. 1–11, 2018.

[7] J. Qi, S. Dalei, C. Wu, J. Han, and T. Wang, "KF-based adaptive UKF algorithm and its application for rotorcraft UAV actuator failure estimation," *International Journal of Advanced Robotic Systems*, vol. 9, no. 4, pp. 1–9, 2012.

[8] R. Kandepu, L. Imsland, and B. A. Foss, "Constrained state estimation using the unscented Kalman filter," *16th Mediterranean Conference on Control and Automation*, 06 2008.

[9] A. Körber and R. King, "Nonlinear model predictive control for wind turbines," in *EWEA*, 2011.

[10] S. Gros, "An economic NMPC formulation for wind turbine control," in *IEEE Conference on Decision and Control*, 2013, pp. 1001–1006.

[11] D. Schlipf, D. J. Schlipf, and M. Kühn, "Nonlinear model predictive control of wind turbines using lidar," *Wind Energy*, vol. 16, pp. 1107–1129, 2013.

[12] S. Gros and A. Schild, "Real-time economic nonlinear model predictive control for wind turbine control," *International Journal of Control*, vol. 90, no. 12, pp. 2799–2812, 2017.

[13] S. Kolås, B. Foss, and T. S. Schei, "State estimation IS the real challenge in NMPC," *Int. Workshop on Assessment and Future Directions of NMPC Pavia, Italy, September 5-9*, 2008.

[14] B. Ritter, A. Schild, and U. Konigorski, "Making nonlinear state estimation techniques ready for use in industrial wind turbine control systems," in *Proceedings of Wind Europe Summit 2016*, 2016.

[15] I. Blanchet, C. Frankignoul, and M. A. Cane, "A comparison of adaptive Kalman filters for a tropical pacific ocean model," *Monthly Weather Review*, vol. 125, pp. 40–58, 1997.

[16] Y. Bar-Shalom, X.-R. Li, and T. Kirubarajan, *Estimation with Applications To Tracking and Navigation*. John Wiley & Sons, 2001.

[17] Z. Chen, C. Heckman, S. Julier, and N. Ahmed, "Weak in the NEES?: Auto-tuning Kalman filters with Bayesian optimization," *CoRR*, vol. abs/1807.08855, 2018.

[18] B. Ritter, E. Mora, and A. Schild, "Observability analysis for horizontal axis wind turbines using empirical Gramian matrices," *Journal of Physics: Conference Series*, vol. 1102, no. 012021, pp. 1–11, 2018.

[19] J. Jonkman and B. Jonkman. (2015) NWTC Information Portal (FAST v8). https://nwtc.nrel.gov/fast8.

[20] B. Ritter, A. Schild, M. Feldt, and U. Konigorski, "The design of nonlinear observers for wind turbine dynamic state and parameter estimation," *Journal of Physics: Conference Series*, vol. 753, no. 052029, pp. 1–12, 2016.

[21] J. Jonkman, S. Butterfield, W. Musial, and G. Scott, "Definition of a 5-MW reference wind turbine for offshore system development," National Renewable Energy Laboratory, Tech. Rep. NREL/TP-500-38060 Feb. 2009, 02 2009.

[22] Q. Song, J. Qi, and J. Han, "An adaptive UKF algorithm and its application in mobile robot control," in *2006 IEEE International Conference on Robotics and Biomimetics*, Dec 2006, pp. 1117–1122.